ISBN: 978-3-95450-184-7 doi:10.18429/JACoW-IPAC2018-WEPMG005

FIRST BEAM TEST OF LASER ENGINEERED SURFACE STRUCTURES (LESS) AT CRYOGENIC TEMPERATURE IN CERN SPS ACCELERATOR

R. Salemme*[1], V. Baglin, S. Calatroni, P. Chiggiato, B. Di Girolamo, E. Garcia-Tabares Valdivieso, B. Jenninger, L. Prever-Loiri, M. Sitko, CERN, Geneva, Switzerland
A. Abdolvand, S. Wackerow, Sch. of Science & Engineering, University of Dundee, Scotland, UK
[1]now at ITER Organization, St. Paul-lez-Durance, France

Abstract

Electron cloud mitigation is an essential requirement for accelerators of positive particles with high intensity beams to guarantee beam stability and limited heat load in cryogenic systems. Laser Engineered Surface Structures (LESS) are being considered, within the High Luminosity upgrade of the LHC collider at CERN (HL-LHC), as an option to reduce the Secondary Electron Yield (SEY) of the surfaces facing the beam, thus suppressing the electron cloud phenomenon. As part of this study, a 2.2 m long Beam Screen (BS) with LESS has been tested at cryogenic temperature in the COLD bore EXperiment (COLDEX) facility in the SPS accelerator at CERN. In this paper, we describe the manufacturing procedure of the beam screen, the employed laser treatment technique and discuss our first observations in COLDEX confirming electron cloud suppression.

INTRODUCTION

The ten-fold increase of luminosity aimed by the High Luminosity upgrade of the LHC (HL-LHC) will impose unprecedented loads to the cryogenic beam vacuum. As a result of an increase of bunch intensity to 2.2×10^{11} ppb, escalation (a factor 5÷7 for $1.2 \leq SEY \leq 1.3$) in heat dissipation is predicted in the inner triplets (IT) and separation dipoles (D1) of IR1/5 and IR2/8 by the extrapolations of the Run 1 and 2 observations [1]. In addition to the concurrent increase of beam impedance contribution, the main heat load is identified in the electron cloud. The cooling budget is presently limited to the ultimate cryogenic capacity of ~200 W. The HL-LHC baseline foresees proactive measures to mitigate electron cloud, by avoidance of the multipacting conditions. Surface treatment will be deployed to reduce secondary electron emission: *ex-situ* in the new HL-LHC triplets for IR1/5, while *in-situ* solutions are developed for IR2/8 by LS3.

The COLD bore Experiment (COLDEX) [2] is experimentally validating, since 2014, the HL-LHC solutions at cryogenic temperature in the Super Proton Synchrotron (SPS) under LHC type beams. Following the 2014-16 campaign, sputtered amorphous carbon (a-C) coating was successfully qualified in COLDEX in HL-LHC operational conditions [3]. a-C coating has proved great maturity and reliable technical feasibility, therefore is considered the HL-LHC baseline. As of 2016, interest has increased in the surface morphology modifications provided by Laser Engineered Surface Structures (LESS) [4, 5] for accelerator applications. This treatment is paving the access to SEY below unity on technical surfaces [6]. The collaboration among CERN, STFC and the University of Dundee (UK) undertook a laboratory and experimental validation campaign, along with a challenging development plan of *in-situ* implementation [7]. Following a first successful accelerator test at room temperature of vacuum components treated with LESS [6], a LHC-type BS was manufactured, laser treated, installed and tested in COLDEX between 2016-17 to qualify LESS performance at cryogenic temperature in accelerator conditions.

MANUFACTURING STRATEGY

A fundamental laser treatment limitation for this work was the maximum treatable length of tubular geometries, capped to 300 mm, due to the available opto-mechanical setup in Dundee. The design and manufacturing of the COLDEX BS, based on single extruded ~2.2 m long, Cu OFE, ID 67 mm circular pipe [2], had to be adapted accordingly (Fig. 1). The BS was divided in nine ID 67/OD 71 mm pipe sections: 8×~245 mm lateral equal segments plus a central, 230 mm long, section accommodating the chimneys ports. Sectioning was performed to maintain the original pattern of LHC-type pumping slots. Once UHV cleaned and passivated, the inner surface of each section was LESS treated. The segments were then assembled by orbital electron beam welding. To achieve a required straightness <0.3 mm/m on the final product, each section had female/male housing/mating lateral shoulders, whose tolerance was H8/f7 (ISO 286) and qualified by metrology. This feature further allowed reducing the heated zone during welding: the electron beam was set to penetrate till the step overlap, affecting only marginally the inner LESS treated surface. Tight prescriptions and specific tooling had to be developed and included in the manufacturing and assembly plan to preserve the treated surface conditions, avoid all contacts and reduce the risk of contaminations. The on-purpose untreated flanges, welded at the BS extremities and in contact with the Cold-to-Warm Transitions, were dry machined-to-length in the final stage of the manufacturing, where the alignment surfaces and points were finally assigned. Apart from the electron beam welding, all assembly processes were conducted in air and in non-clean room classified environment.

LASER TREATMENT

The laser surface structuring was performed using a linearly polarized pulsed (10 ps) laser system operating at wavelength of 532 nm and repetition rate of 200 kHz. The laser beam had a Gaussian intensity profile (M^2<1.3). The

* roberto.salemme@iter.org

Content from this work may be used under the terms of the CC BY 3.0 licence (© 2018). Any distribution of this work must maintain attribution to the author(s), title of the work, publisher, and DOI.
This is a preprint — the final version is published with IOP

ISBN: 978-3-95450-184-7 doi:10.18429/JACoW-IPAC2018-WEPMG005

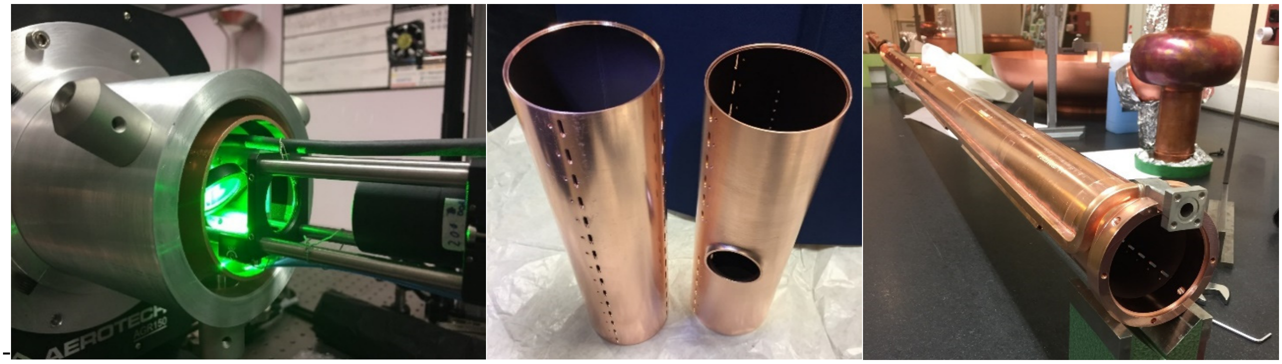

Figure 1: Manufacturing phases (left to right): LESS treatment, lateral and central treated segments, final assembled BS.

diameter of the focused spot, measured between the points where the intensity falls to *1/e*^{2} of the central value, was calibrated to ~13 µm prior start of each laser structuring. The depth of focus – the distance either side of the beam waist determining a beam diameter grow by 5% – was estimated ~60 µm. Laser treatment was performed with a fixed laser system. Each BS segment was installed on a gear-driven rotary stage, itself mounted on a precision ball-screw linear stage, both driven by brushless servomotors. Prior to laser treatment, the entire inner surface of each BS segment was scanned, by rotation at 100 °/s, using a laser-optical displacement sensor to obtain the surface profile. This was used during the laser structuring to adjust the focusing distance by an *in-house* designed automated optical system. The extrusions presented by the BS chimneys ports could be partially treated thanks to this automatism. The treatment was performed in air at room temperature, under a ~3 l/min blow of N_2 flowing at the laser focus point. The structures were obtained writing a line pattern along the pipe circumference. The resulting pattern is Line Hatched (LH), perpendicular to the pipe (and accelerator proton beam) axis. The rotating (17 °/s) stage assured a surface scanning speed of 10 mm/s leading to approximately 240 pulses being fired per spot. Obtained a full circle, the linear stage stepped such that the distance between consecutive lines was kept at ~24 µm. In such configuration, the total laser processing accounted ~60 h/segment. The experimentally assessed ablation depth was 36±6 µm [6]. The LESS treatment was performed at average laser pulse energy of 5 µJ (laser beam intensity of ~0.4 TW·cm^{-2}). Negligible heat deposition, consequently no thermal deformation, was observed.

PRE-SERIES CHARACTERIZATION

Samples obtained by destructive methods from pre-series BS LESS segments, treated according to the developed methodology, were surface characterized. Based on the phenomenological modeling of the SEY energy dependence, δ(E), described in [8] and [9], in the window R_0 = [0.7:1.0] and for an arbitrary E_0 = 150 eV, the following SEY parameters were measured at room temperature: $\delta_{max} \approx 0.87$, $E_{max}(\delta_{max}) \approx 861$ eV, s ≈ 1.19. Compared to Cu ($E_{max} \approx 200$ eV, s ≈ 1.35 when conditioned) and a-C coatings ($E_{max} \approx 270$ eV, s ≈ 1.75), the measured δ(E) laid entirely below the unity and its energy dependence had a smoother peak (s closer to unity), shifted to higher energies, as expected [5, 6]. The same study was repeated on two, 2 mm thick, Cu OFE strips, butt welded with 100% penetration after LESS treatment. The analysis revealed no significant increase in surface SEY far from the weld. A marginal increase was measured on the zones impacted by heat and copper projections during the weld. In these portions, the XPS analysis showed an increase (< 40%) of C1s peak. Overall, the XPS spectrum indicated absence of any other significant surface elemental modification or contamination. Electron beam welding was not impairing the overall UHV quality of the assembled BS surfaces. Considering the partial penetration set to weld the BS segments and the intrinsic transversal nature of beam induced multipacting, the presence of delimited (about 2% by surface) portions of degraded SEY was expected by design and deemed acceptable. The positive feedback obtained by pre-characterization validated the series treatment. During the production phase, tight follow-up of the laser parameters was ensured for quality assurance.

ACCEPTANCE TESTS

Vacuum qualification and pre-acceptance tests of two LESS treated segments were carried before their final welding. Their vacuum pump-down exhibited a linear behaviour in logarithmic time/total pressure scale, with slope of -0.75. This pointed to presence of high roughness and open porosity. The specific H_2O outgassing rate at 10 h was ~1×10^{-8} mbar·l·s^{-1}·cm^{-2}, ~30 times the reference for unbaked, untreated, copper. A decrease of about half from results obtained on the first batch of LESS treated surfaces dating back to 2016 [6] was noted. The Residual Gas Analysis after 24 h of pumping was readily within CERN acceptance criteria for unbaked components [10]. The same tests were conducted on the welded strips with similar, satisfactory results. Both studies proved preservation of cleanliness and fitness to UHV performance.

At reception, the full welded BS was dressed with a new, calibrated, CERNOX™ temperature sensor, 23 BS pumping slot shields (untreated), the BS electrode (untreated), the fixed point plate, the gravity support screws. The same 316LN stainless steel grids (geom. transparency: ~0.56) used in 2003-16 were mounted on the new BS chimneys ports to ensure consistency. Following the short circuits suffered in 2014-16 cryogenic operation [3], ascribed to a

This is a preprint — the final version is published with IOP
Content from this work may be used under the terms of the CC BY 3.0 licence (© 2018). Any distribution of this work must maintain attribution to the author(s), title of the work, publisher, and DOI.

ISBN: 978-3-95450-184-7 doi:10.18429/JACoW-IPAC2018-WEPMG005

loss of alignment due to differential thermal contractions, the BS electrode insulation was improved by manufacture of ID 2 mm alumina bushes. The assembled BS was then inserted in a vacuum test bench. Fluid feedthroughs to the cooling circuit flanges were connected to allow cryogenic cool-down. The vacuum pump-down exhibited a slope of -0.737. The total measured outgassing at 10 h was 3.8×10^{-8} mbar·l·s^{-1}. Excluding the reference contribution of the Cu unbaked untreated surfaces, the LESS specific H_2O outgassing rate was ~27 times more, in line with the single segment configuration. The RGA analysis after 13 h of pumping revealed only a slight (< 2‰ the main H_2O peak) hydrocarbon contamination of amu >50. The amount was reducible with prolonged pump-down and this prevented the option of vacuum bake-out, which would have spoiled representativity of the test. Considering the challenging manufacturing process and methods, the vacuum quality of the final product passed all acceptance tests. The BS was finally thermally conditioned in HV conditions one time by cool-down at LN_2 temperature. A concurrent read-out of the BS electrode validated its upgraded design.

BEAM OBSERVATIONS

The first COLDEX experimental SPS beam run with LESS took place in July 2017. The BS and Cold Bore (CB) were cryogenic cooled down ten days before the run (after ~2200 h of vacuum pumping). Five days before the run, the low accumulated gas coverage on the BS surface was regenerated twice to 120 K. The gas released in three main peaks: one due to H_2 above 15 K, followed by N_2, O_2, Ar, CO above 20 K, and CO_2 above 63 K. This desorption pattern points to a weaker spectrum of energies for desorption than a-C [3], more similar to bare Cu. Further, the presence of a negligible but measurable amount of air in the system, not detectable by RGA without accumulation, is noted. Over a 23-hours beam runtime, the accumulated beam dose exceeded 1.5 Ah. Two BS temperatures have been chosen: first 10 K, raised to 60 K in the second part of the run. The CB was kept permanently at 2.7 K. The SPS intensity was ramped-up progressively from one to four batches of 72 bunches, 25 ns spaced, of 1.0×10^{11} ppb at 26 GeV/c. Multipacting was detected at COLDEX stainless steel extremities at RT (initial SEY ≈1.9), by pressure rises up to ~5×10^{-7} mbar. The main desorbed gases were, in order, H_2, CO, CO_2. The application of ~0.5 mT solenoidal magnetic field mitigated the electron multipacting in these regions. No pressure increase due to beam stimulated desorption was instead measured (detection limit: 10^{-10} mbar) in COLDEX. The gas composition, dominated by the background H_2, was stable throughout the runtime at 10 K. At 60 K, H_2 transmitted from the extremities and not physisorbed on LESS was instead measurable. Within the detection limit (~100 mW/m), no dynamic heat load was measured in COLDEX. This was insensitive to the number of beam batches (1 to 4×72 bunches, 25 ns). The temporary increase to 1.5×10^{11} ppb or decrease to 0.7×10^{11} ppb did not alter the observation. Electron cloud heat load was suppressed thanks to the surface SEY below the multipacting threshold (1.2-1.3 with Cu in COLDEX). The resistive wall contribution of the beam impedance was below measurement limit, as expected by simulation. When calculated in IW2D [11], with a multilayer model including a LESS layer 8 μm thick and resistive 13 times more than Cu (RRR=80) [12], the resistive wall power loss is estimated dissipating ~10 mW/m in COLDEX with a nominal (1.3×10^{11} ppb, 3 ns 4σ bunch length) LHC-type beam.

The chimney electrode confirmed the results from the heat load measurements. Signal was below detection limit (10^{-10} A) and insensitive to the number of batches or the bunch intensity. The BS electrode showed instead electron activity with positive bias: up to 10^{-7} A were measured with +1 kV and 4×72 bunches (1.0×10^{11} ppb). The electron current was sensitive to the number of batches and bunch intensity, *i.e.* proportional to the circulating intensity, but lower by at least two decades to what measured in multipacting conditions with similar beam intensity [13]. Voltage sweeps enabled electron spectral observations. A peaked spectrum of electron was detectable between 0 and +100 V, followed by a flat trend that corresponds to a linearly increasing amount of electrons collected when rising bias above +100 V. Volume collection efficiency was proportional to the applied bias. The application of a negative voltage returned a constant pedestal value not correlated to the beam intensity, excluding presence of beam image current. To verify the correct operation of the chimney electrode, a pressure bump was induced during beam circulation of 4×72 bunches (1.0×10^{11} ppb) at the end of the run, by raising the BS temperature to 60 K. The thermal desorption of mainly H_2 induced a twenty-two-fold peak increase of vacuum density, readily observed as a proportional increase of measured current on both the chimney and BS electrodes. This correlated the reading with the primary electron source, which is beam residual gas ionization in COLDEX.

CONCLUSIONS

LESS surface treatments have the potential to eradicate electron multipacting in high intensity positively charged accelerators and storage rings. A LESS treated surface was beam tested for the first time at cryogenic temperature in COLDEX. The challenge involving the treatment of the beam facing surfaces prior to their mechanical assembly was tackled by a manufacture procedure and pre-characterization which demonstrated preservation of the surface SEY within UHV requirements. Throughout the beam operation, the COLDEX vacuum, heat load and electron measurements show that electron multipacting is efficiently mitigated (suppressed in COLDEX) by LESS at cryogenic temperature. The expected increase in resistive wall beam impedance heating was contained and had no effect in COLDEX; however, this mechanism shall be pondered for application of this technology to accelerator beams of shorter bunch length and higher bunch intensity. The BS electrode readings, obtained for the first time in COLDEX in absence of multipacting, will be the subject

Content from this work may be used under the terms of the CC BY 3.0 licence (© 2018). Any distribution of this work must maintain attribution to the author(s), title of the work, publisher, and DOI.
This is a preprint — the final version is published with IOP

ISBN: 978-3-95450-184-7 doi:10.18429/JACoW-IPAC2018-WEPMG005

of further analysis and new dedicated studies, along with beam experimental runs with pre-adsorbed gas species.

ACKNOWLEDGMENTS

The laser structuring work was conducted *in-house* at the University of Dundee under the aegis of grants and financial support from the STFC (Grant No. ST/P00086X/1) and CERN (Collaboration Agreement KN3362). The support of the CERN EN-MME central workshop team, I. Wevers and C. Vazquez Pelaez during, respectively, the BS manufacture, characterization and installation is warmly acknowledged.

REFERENCES

[1] G. Iadarola, E. Metral, and G. Rumolo, CERN Report No. CERN-ACC-2016-0112, 2016.

[2] R. Salemme *et al.*, "Recommissioning of the COLDEX experiment at CERN", in *Proc. IPAC'15*, Richmond, VA, USA, May 2015, paper WEPHA006, pp. 3109-3111.

[3] R. Salemme *et al.*, "Vacuum performance of amorphous carbon coating at cryogenic temperature with presence of proton beams", in *Proc. IPAC'16*, Busan, Korea, May 2016, paper THPMY007, pp. 3663-3666.

[4] G. Tang *et al.*, "Nanosecond pulsed laser blackening of copper", *Appl. Phys. Lett.*, vol. 101, p. 231902, 2012.

[5] R. Valizadeh *et al.*, "Low secondary electron yield engineered surface for electron cloud mitigation", *Appl. Phys. Lett.*, vol. 105, p. 231605, 2014.

[6] S. Calatroni *et al.*, "First accelerator test of vacuum components with laser-engineered surfaces for electron-cloud mitigation," *Phys. Rev. Accelerators & Beams*, vol. 20, p. 113201, 2017.

[7] M. Sitko *et al.*, "Towards the implementation of Laser Engineered Surface Structures for electron cloud mitigation", presented at IPAC'18, Vancouver, Canada, Apr.-May 2018, paper TUZGBE3, this conference.

[8] M. A. Furman, M. Pivi, "Probabilistic model for the simulation of secondary electron emission", *PRST-AB*, vol. 5, p. 12404, 2002.

[9] R. Cimino *et al.*, "Can low-energy electrons affect high-energy physics accelerators?", *Phys. Rev Lett.*, vol. 93, no. 1, p. 014801, 2004.

[10] "Procédure d'acceptation de composants pour les systèmes à vide des injecteurs non étuvés du LHC", CERN EDMS 1437531, 2014.

[11] N. Mounet, E. Métral, "Electromagnetic fields and beam coupling impedances in a multilayer flat chamber", CERN-ATS-Note-2010-056 TECH, 2010.

[12] S. Arsenyev, S. Calatroni (CERN), private communication.

[13] V. Baglin, B. Jenninger, "Pressure and heat load in a LHC type cryogenic vacuum system subjected to electron cloud", *Proc. ECLOUD'04*, AIP Conf Proc. 773, CERN-2005-001, 2005.

This is a preprint — the final version is published with IOP

Content from this work may be used under the terms of the CC BY 3.0 licence (© 2018). Any distribution of this work must maintain attribution to the author(s), title of the work, publisher, and DOI.